Ultrafast terahertz-induced response of GeSbTe phase-change materials

Michael J. Shu,[1,2,a)] Peter Zalden,[2,3] Frank Chen,[2,4] Ben Weems,[5] Ioannis Chatzakis,[2] Feng Xiong,[4] Rakesh Jeyasingh,[4] Matthias C. Hoffmann,[6] Eric Pop,[4] H.-S. Philip Wong,[4] Matthias Wuttig,[7,8] and Aaron M. Lindenberg[2,3,5,b)]

[1]*Department of Applied Physics, Stanford University, Stanford, California 94305, USA*
[2]*Stanford Institute for Materials and Energy Sciences, SLAC National Accelerator Laboratory, Menlo Park, California 94025, USA*
[3]*PULSE Institute, SLAC National Accelerator Laboratory, Menlo Park, California 94025, USA*
[4]*Department of Electrical Engineering, Stanford University, Stanford, California 94305, USA*
[5]*Department of Materials Science and Engineering, Stanford University, Stanford, California 94305, USA*
[6]*SLAC National Accelerator Laboratory, Menlo Park, California 94025, USA*
[7]*I. Physikalisches Institut, RWTH Aachen University, 52056 Aachen, Germany*
[8]*JARA–Fundamentals of Information Technology, RWTH Aachen University, 52056 Aachen, Germany*

The time-resolved ultrafast electric field-driven response of crystalline and amorphous GeSbTe films has been measured all-optically, pumping with single-cycle terahertz pulses as a means of biasing phase-change materials on a sub-picosecond time-scale. Utilizing the near-band-gap transmission as a probe of the electronic and structural response below the switching threshold, we observe a field-induced heating of the carrier system and resolve the picosecond-time-scale energy relaxation processes and their dependence on the sample annealing condition in the crystalline phase. In the amorphous phase, an instantaneous electroabsorption response is observed, quadratic in the terahertz field, followed by field-driven lattice heating, with Ohmic behavior up to 200 kV/cm. © 2014 AIP Publishing LLC. [http://dx.doi.org/10.1063/1.4884816]

Phase change materials (PCMs) have been studied for use in nonvolatile memory devices due to their fast electrically-induced switching between a high-resistance amorphous phase and a low-resistance crystalline phase.[1,2] The field-driven heating of the material is essential to the switching process, although alternative switching mechanisms have also been proposed recently.[3–6] In the standard picture, crystallization occurs when the amorphous material is heated above the crystallization temperature, often on a nanosecond time-scale. This is assisted by a "threshold switching" mechanism in which the conductivity of the amorphous phase increases sharply at a threshold applied electric field around 500 kV/cm.[7–12] For amorphization, the temperature is raised beyond the melting temperature and quenched rapidly. Understanding the electric field response of these materials is important for predicting the field-driven heating and phase-change behavior. However, it is difficult to determine the nature of electrical conduction in either phase using conventional electrical bias measurements, which involve applying a voltage across a PCM cell and measuring the resulting current. This method has limitations in the speed at which voltage pulses may be applied and currents measured, making it difficult to resolve the initial steps of the electrically driven response, which occur on ultrafast time-scales governed by electron-phonon coupling and relaxation processes. External circuits can complicate the interpretation of measurements by introducing resistive and capacitive contributions separate from the PCM. Here, we make use of single-cycle terahertz-frequency (THz) light pulses as an all-optical means of applying large amplitude picosecond electric

field pulses to materials, with electric field magnitude comparable to relevant switching fields. This allows the possibility of electrically biasing PCM samples on time-scales shorter than energy relaxation processes and without the need for electrical contacts or circuits, in contrast to both nanosecond electrical bias and above-bandgap photoexcitation techniques.

The initial steps in the field-driven response are closely associated with the nature of electrical transport in the materials. Numerous models attempt to explain the conduction mechanisms in amorphous PCMs.[7–13] For example, Ielmini and Lacaita have measured and modeled the field dependent conduction in PCMs for steady state conditions, with results signifying both a Poole-Frenkel and phonon-assisted tunneling mechanism for conduction in the amorphous phase.[14] Siegrist *et al.* have investigated electrical transport in the crystalline phase, using static electrical measurements to characterize the progression of the electrical properties with increasing annealing temperature.[15] Conduction mechanisms were associated with localized charge carriers in the low annealing temperature, highly disordered crystalline state, transitioning to delocalized carriers at higher annealing temperatures, thereby undergoing a disorder-driven insulator-metal transition. Breznay *et al.* have measured disorder-dominated transport even in the metallic phase.[16]

GeSbTe (GST) alloys are widely used and of technological importance for phase-change applications. We have employed a pump-probe measurement scheme to determine the time-resolved response of GST films to THz electric fields.[17] We pumped the films with THz pulses—less than 1 ps pulse width and peak field strength of order 100 kV/cm—and measured the near-bandgap transmission through the films, as a time-resolved probe of the induced thermal and electronic effects below the switching threshold. The THz

---

[a)]M. J. Shu and P. Zalden contributed equally to this work.
[b)]Electronic mail: aaronl@stanford.edu

pulses were generated using a tilted pulse front scheme employing optical rectification in a LiNbO$_3$ crystal.[18] The near-infrared probe pulses of $\sim$50 fs duration were generated by an optical parametric amplifier. The two beams were focused collinearly on the sample surface with a THz spot size of 1.5 mm and a probe spot size of 400 μm. The samples under investigation were a 230 nm thick sputter-deposited crystalline film of GeSb$_2$Te$_4$ on a glass substrate, which had been annealed at 300 $^\circ$C under inert conditions, and a 1.6 μm thick as-deposited amorphous film of Ge$_2$Sb$_2$Te$_5$ on a Si substrate. Measurements were also performed as a function of sample annealing temperature on a 500 nm Ge$_2$Sb$_2$Te$_5$ film on glass.

The near-infrared transmission spectra of the materials were first measured in a Fourier-transform infrared spectrometer (FTIR), around the tails of the absorption spectrum.[19] Figs. 1(a) and 1(b) reveal the static temperature-dependence of the transmission spectra for crystalline and amorphous GST, respectively. The temperature-dependent measurements were taken during sample cooling beginning at the highest temperature. The transmission of both phases decreases across the spectrum as temperature is increased, corresponding to a redshift of the edge; the reduction scales linearly with temperature, consistent with established models and previous experiments.[20,21] The temperature-induced change in transmission is strongest at or above the band gap—about 0.8 eV in the amorphous phase and 0.5 eV in the crystalline phase.

Fig. 2 shows the THz electric-field driven response of crystalline GeSb$_2$Te$_4$ film, which is in the highly conducting, stable crystalline phase. The time-resolved fractional modulation of infrared transmission, $\Delta\tau/\tau$, is plotted in Figs. 2(a) and 2(b) for 2.5 μm (0.5 eV, near the bandgap) and 1.5 μm (0.83 eV, above the bandgap) probe wavelength, respectively, with a peak THz field strength of 50 kV/cm. At 0.5 eV, the THz pulse causes a decrease in transmission, which decays on a few picosecond time-scale. At 0.83 eV, the transmission gradually decreases during the few picoseconds following THz excitation, and an extrapolation of the present data indicates that it remains at the reduced value for at least 0.4 ns.

We explain this result in terms of the carrier and lattice dynamics induced by ultrafast electric-field excitation. The THz electric field couples to charge carriers, and for crystalline GST—a degenerate p-type semiconductor[15]—this creates hot carriers in states near the valence band edge. Absorption at 0.5 eV is associated with transitions from these near-edge states and, consequently, is enhanced when hot electrons occupy states above the Fermi level, which can be associated with a Burstein shift of the edge (Fig. 2(a), insets).[22,23] Estimates of the electric field induced broadening of the absorption edge due to Franz-Keldysh effects are on the order of 10^{-4} and can be ruled out as a significant contribution to the time-zero response.[19,24,25] This is consistent with previous observations in which the effect of hot carriers was found to be more important than the Franz-Keldysh effect in producing a modulation in absorption for degenerate semiconductors.[23] Moreover, the gradual decay after the peak clearly does not result from an instantaneous field-driven response. The time-resolved response at 0.5 eV, therefore, probes the temperature of the electronic system and its relaxation dynamics. In addition to hot carriers, the lattice temperature also influences the transmission through the film as in Fig. 1. Since 0.83 eV is high above the crystalline band gap, absorption at this probe energy is insensitive to the hot carriers generated by the THz pulse, and the measurement at 0.83 eV is instead dominated by the lattice heating response, associated with a long-lived decrease in transmission decaying on thermal transport time-scales. We note that the lattice heating effect is also seen at 0.5 eV, as a long-lived reduction in transmission, which is weak compared to the fast hot carrier-driven response.

We model the response of the crystalline phase by using a two-temperature model to describe the response of the electron and lattice temperatures to the applied THz pulse.[26] The response of the electronic temperature T_e and the lattice temperature T_i as a function of time t are given by

$$C_e \frac{dT_e}{dt} = -G(T_e - T_i) + \sigma E^2(t), \qquad (1a)$$

$$C_i \frac{dT_i}{dt} = G(T_e - T_i), \qquad (1b)$$

where C_e and C_i are the electronic and lattice specific heats, respectively, G is the electron-lattice coupling coefficient, σ is the conductivity, and $E(t)$ is the instantaneous electric field. In this model, the electrons are Joule-heated by the instantaneous THz field; energy is then transferred from the hot electron system to the lattice. The effect of lattice heating on the film transmission is determined from the temperature-dependent FTIR measurements. The transmission change at 0.83 eV is modeled to follow the lattice temperature rise, whereas the transmission change at 0.5 eV is due to the lattice temperature rise as well as the Burstein shift $4kT_e$ of the absorption edge resulting from hot carriers.[23] The fit results are shown as dark lines in Figs. 2(a) and 2(b), and the corresponding electronic and lattice temperatures are plotted in Fig. 2(c) along with the THz waveform. From the fit, we extract an electron-lattice coupling time of 0.8 $\pm$ 0.1 ps, similar to previously measured energy relaxation time-scales for photoexcited carriers in GeSb$_2$Te$_4$.[27] The long-lived decrease in transmission at 0.83 eV has a lifetime of at least 0.4 ns, reflecting the time for thermal diffusion into the substrate. As shown in Fig. 3, with THz fields up to 50 kV/cm, we observe that the magnitude of the transmission modulation at 0.5 eV scales linearly with the THz intensity (quadratically with electric field), as expected for a Joule heating
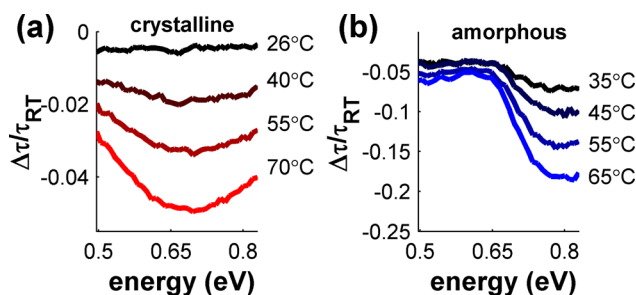

FIG. 1. (a) Temperature dependent change in transmission τ through 50 nm crystalline GST on glass substrate from 26 $^\circ$C to 70 $^\circ$C, normalized with respect to room-temperature transmission τ_{RT}. (b) Temperature dependent change in transmission through 250 nm amorphous GST on Si substrate from 35 $^\circ$C to 65 $^\circ$C.
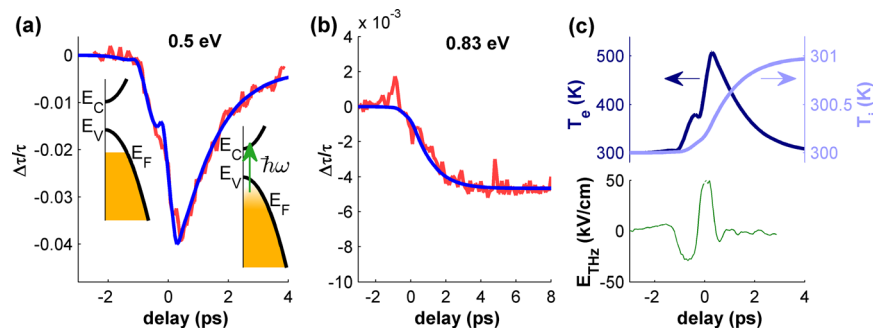
FIG. 2. Response of crystalline Ge$_1$Sb$_2$Te$_4$ with THz pump. Time-resolved fractional transmission modulation $\Delta\tau/\tau$ is shown at (a) 0.5 eV and (b) 0.83 eV. Red: data; blue: fit from two-temperature model. The band schematic is shown as insets in (a), with occupied electron states shaded. Left inset: before time zero. Right inset: upon THz excitation, the carriers heated by the THz pulse move to states closer to the band edge and can absorb photons with energy near the bandgap. (c) Two-temperature model results (dark line: electronic temperature; light line: lattice temperature) and THz waveform (bottom).

effect with a constant conductivity (Eq. (1a)). With a peak field strength of 50 kV/cm, we drive a lattice temperature jump of 1.0 K.

Measurements were performed as a function of sample annealing temperature in order to investigate the dependence of the observed dynamics on the sample structural phase. Fig. 4(a) shows the time-resolved transmission at 0.5 eV for a GST sample in the as-deposited amorphous phase, and annealed at 170 °C, 250 °C, and 325 °C.[19] The conductivity and atomic ordering of the GST increases as the sample is annealed at higher temperatures.[15] No time-resolved effect is seen in the amorphous phase because the probe energy is well below the band gap. In each crystalline phase, a decrease in transmission is observed during the peaks of the THz field, with a recovery afterward. Fig. 4(b) shows the electronic temperature response obtained from a two-temperature model fit for each annealing temperature.[19] The electron energy relaxation rate is significantly faster in the 170 °C crystalline phase (<0.2 ps) than in either higher temperature phase (both 1.0 ± 0.1 ps). This gives a general trend of slower energy relaxation as the phase-change sample is annealed at higher temperatures, corresponding to increased crystalline order. This is consistent with the increasing conductivity of the higher-temperature phases, which implies slower electron scattering rates. We also see a stronger effect with higher annealing temperature, again reflecting the

increasing conductivity and, hence, increasing magnitude of field-driven carrier heating (Eq. (1a)).

The optical response of amorphous Ge$_2$Sb$_2$Te$_5$ upon THz electric field excitation is shown in Fig. 5(a). The peak field strength is 200 kV/cm, and the probe wavelength is 1.5 μm (0.83 eV). The field strength of the pump pulse is in a regime where non-Ohmic behavior is typically observed in DC measurements,[13] but below the field strength necessary to trigger the threshold switching process.[12] The amorphous phase shows a transient decrease in transmission, which follows the rectified THz waveform and is proportional again to the square of the field (Fig. 5(b)). The small positive signal between the two negative peaks was determined to originate from the Si substrate. The instantaneous response is consistent with previous electroabsorption studies in amorphous semiconductors, scaling quadratically with the field.[19,24,28,29] Because the Fermi level lies within the energy gap for the amorphous phase,[14] the role of hot carrier effects can likely be ruled out.

Following the pump pulse, there is also a long-lived decrease in transmission (see Fig. 5(a), inset). The long-lived effect decays on a nanosecond time-scale and is most likely due to heating of the lattice. We note that the electron-lattice coupling must be faster in the amorphous phase compared to the crystalline phase because the long-lived response is already present at the end of the THz pulse, whereas the modulation took ~2 ps to fully develop in the crystalline phase (Fig. 2(b)). Fig. 5(c) shows the THz intensity dependence of the long-lived effect. The peak fields used here—up to 200 kV/cm—are below the values required for threshold switching with longer pulses.[8,12] The long-lived effect also scales with the square of the THz field, which indicates a constant conductivity and thus an Ohmic response over the full range of electric fields investigated here (Eq. (1a)). This suggests that the non-Ohmic behavior observed in previous DC electrical bias measurements at similar fields is an effect that builds up on longer time-scales. The maximum long-lived modulation corresponds to a temperature jump of 0.01 K for a peak field strength of 200 kV/cm according to comparison with FTIR data.

These measurements of the ultrafast electric field response of GST shed light on the initial steps in the field-driven phase change processes for these materials. The electric field-driven heating process is measured with a
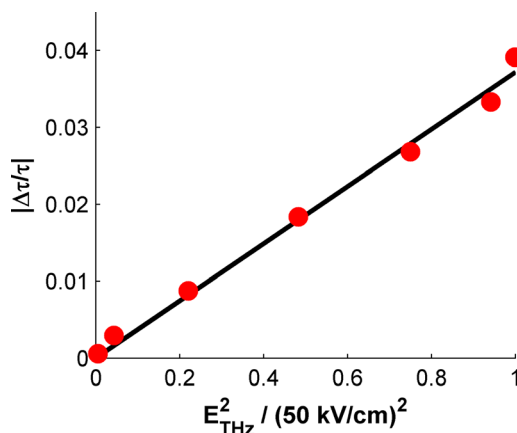

FIG. 3. THz intensity dependence of the peak transmission modulation $\Delta\tau/\tau$ in crystalline Ge$_1$Sb$_2$Te$_4$ at 0.5 eV. Red circles: data. Black line: linear fit.
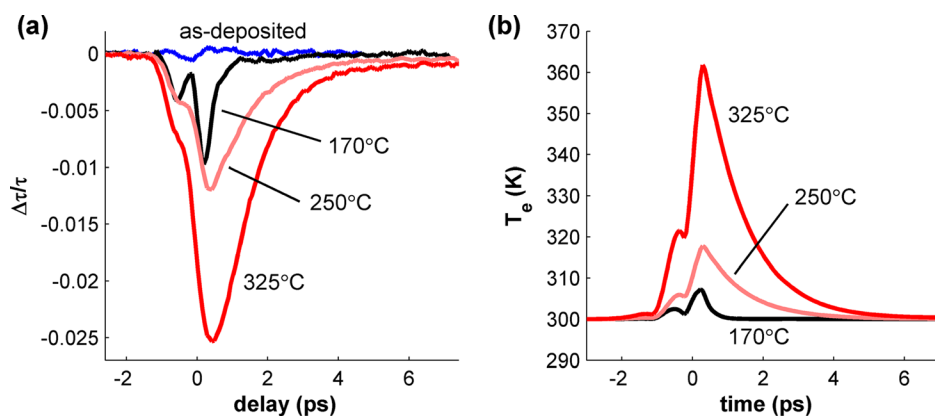
FIG. 4. (a) Time-resolved transmission modulation $\Delta\tau/\tau$ in $Ge_2Sb_2Te_5$ for different annealing temperatures. Blue: as-deposited amorphous; black: 170 °C; pink: 250 °C; red: 325 °C. (b) Electronic temperature response from two-temperature model.
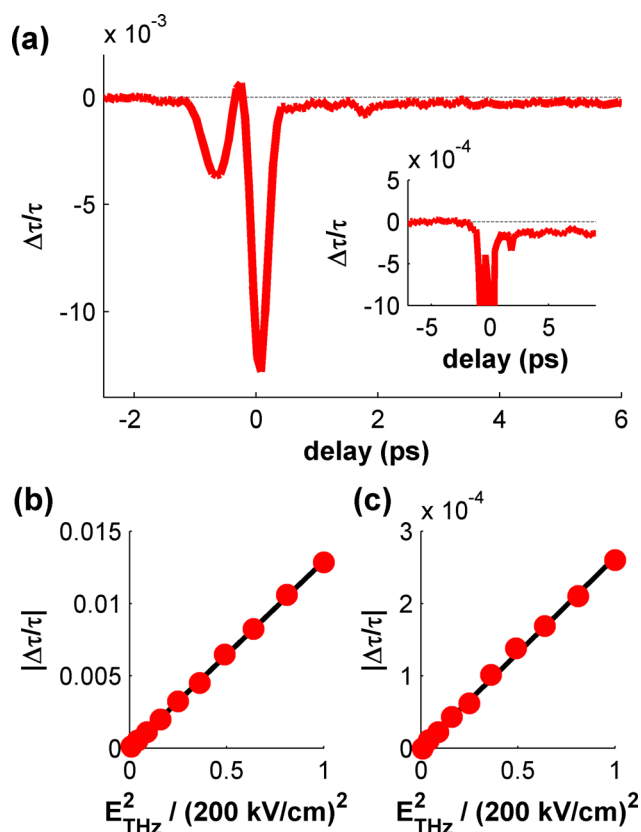

FIG. 5. (a) Time-resolved transmission modulation $\Delta\tau/\tau$ of amorphous $Ge_2Sb_2Te_5$ at 0.83 eV with THz pump at 200 kV/cm peak field. Inset: the response expanded to show the long-lived reduction in transmission. (b) THz intensity dependence of the peak time zero effect. (c) THz intensity dependence of the long-lived effect. Red circles: data. Black line: linear fit.

pump pulse shorter than or comparable to the heating time. This enables direct observation of carrier heating processes and the energy transfer from hot carriers to the lattice for both crystalline and amorphous phases and as a function of annealing temperature, showing faster relaxation processes for more disordered samples. These measurements additionally identify Joule-heating processes as the dominant mechanism for field-induced temperature jumps in GST. Future measurements at higher applied fields may enable extraction of the ultimate time-scales for the switching process itself.

[1]A. Pirovano, A. L. Lacaita, A. Benvenuti, F. Pellizzer, and R. Bez, IEEE Trans. Electron Devices **51**, 452 (2004).

[2]H.-S. P. Wong, S. Raoux, S. Kim, J. Liang, J. P. Reifenberg, B. Rajendran, M. Asheghi, and K. E. Goodson, Proc. IEEE **98**, 2201 (2010).

[3]K. Sokolowski-Tinten, J. Solis, J. Bialkowski, J. Siegel, C. N. Afonso, and D. von der Linde, Phys. Rev. Lett. **81**, 3679 (1998).

[4]A. V. Kolobov, M. Krbal, P. Fons, J. Tominaga, and T. Uruga, Nat. Chem. **3**, 311 (2011).

[5]K. Makino, J. Tominaga, A. V. Kolobov, P. Fons, and M. Hase, Appl. Phys. Lett. **101**, 232101 (2012).

[6]D. Loke, T. H. Lee, W. J. Wang, L. P. Shi, R. Zhao, Y. C. Yeo, T. C. Chong, and S. R. Elliott, Science **336**, 1566 (2012).

[7]D. Adler, H. K. Henisch, and N. F. Mott, Rev. Mod. Phys. **50**, 209 (1978).

[8]D. Ielmini and Y. Zhang, J. Appl. Phys. **102**, 054517 (2007).

[9]D. Ielmini, Phys. Rev. B **78**, 035308 (2008).

[10]H. Fritzsche, J. Phys. Chem. Solids **68**, 878 (2007).

[11]V. G. Karpov, Y. A. Kryukov, S. D. Savransky, and I. V. Karpov, Appl. Phys. Lett. **90**, 123504 (2007).

[12]D. Krebs, S. Raoux, C. T. Rettner, G. W. Burr, M. Salinga, and M. Wuttig, Appl. Phys. Lett. **95**, 082101 (2009).

[13]M. Nardone, M. Simon, I. V. Karpov, and V. G. Karpov, J. Appl. Phys. **112**, 071101 (2012).

[14]D. Ielmini and A. L. Lacaita, Mater. Today **14**, 600 (2011).

[15]T. Siegrist, P. Jost, H. Volker, M. Woda, P. Merkelbach, C. Schlockermann, and M. Wuttig, Nat. Mater. **10**, 202 (2011).

[16]N. P. Breznay, H. Volker, A. Palevski, R. Mazzarello, A. Kapitulnik, and M. Wuttig, Phys. Rev. B **86**, 205302 (2012).

[17]T. Kampfrath, K. Tanaka, and K. A. Nelson, Nat. Photonics **7**, 680 (2013).

[18]J. Hebling, K.-L. Yeh, M. C. Hoffmann, B. Bartel, and K. A. Nelson, J. Opt. Soc. Am. B **25**, B6 (2008).

[19]See supplementary material at http://dx.doi.org/10.1063/1.4884816 for room-temperature infrared transmission spectra, a discussion of electroabsorption, x-ray diffraction patterns for different annealing temperatures, and details of the two-temperature model.

[20]Y. P. Varshni, Physica **34**, 149 (1967).

[21]S. Kremers, Ph.D. thesis, RWTH Aachen University, Aachen, Germany, 2009.

[22]E. Burstein, Phys. Rev. **93**, 632 (1954).

[23]M. S. Shur, Phys. Lett. A **29**, 490 (1969).

[24]W. Franz, Z. Naturforsch. **13a**, 484 (1958).

[25]F. Novelli, D. Fausti, F. Giusti, F. Parmigiani, and M. Hoffmann, Sci. Rep. **3**, 1227 (2013).

[26]M. Liu, H. Y. Hwang, H. Tao, A. C. Strikwerda, K. Fan, G. R. Keiser, A. J. Sternbach, K. G. West, S. Kittiwatanakul, J. Lu, S. A. Wolf, F. G. Omenetto, X. Zhang, K. A. Nelson, and R. D. Averitt, Nature **487**, 345 (2012).

[27]M. J. Shu, I. Chatzakis, Y. Kuo, P. Zalden, and A. M. Lindenberg, Appl. Phys. Lett. **102**, 201903 (2013).

[28]B. T. Kolomiets, T. F. Mazets, S. M. Efendiev, and A. M. Andriesh, J. Non-Cryst. Solids **4**, 45 (1970).

[29]G. Weiser, U. Dersch, and P. Thomas, Philos. Mag. B **57**, 721 (1988).